International Journal of ChemTech Research
CODEN (USA): IJCRGG ISSN: 0974-4290
Vol.9, No.03 pp 431-443, 2016

Enhance photocatalytic Activity of TiO_2 by Carbon Nanotubes

Firas H. Abdulrazzak

Chemistry Department, College of Education for Pure Sciences, Diyala University, Diyala, Iraq

Abstract: Two types of composites consisting of single –walled carbon nanotubes (SWNTs) and mwuti-walled carbon nanotubes (MWNTs) with titanium dioxide (TiO_2-P25) were synthesized by simple evaporation methods. These composites were characterized by UV–vis diffuse reflectance, XRD, Raman spectroscopy, Fluorescence spectroscopy and Surface area (S_{BET}). The results show that Carbon Nanotubes (CNT) which used to synthesis composites (TiO_2/CNTs) has succeeded in increased the activity of $TiO_2$when exhibits higher photocatalytic activity than TiO_2.The multi walled carbon nanotubes MWNTs were succeeded to increase the adsorption for synthesis composites more than SWNTs, while SWNTs succeed to improve the activity of photocatalytic degradation of TiO_2. The enhancements of the activity for the composites by the two types of CNTs can explain by two parameters: the first were increased the surfaces area for synthesis composites and the second was translating the exited electron e^- from conduction bands (CB) of TiO_2 to the surfaces of CNTs which causing reduces the recombination of e^-/h^+.
Keywords: SWNT, MWNT, P25, TiO_2/CNTs composite, Cobalamin degradation, out situ activity.

1-Introduction

Titanium dioxide (TiO_2) has long been a promising material for photocatalysis applications due to environmentally friendly and relatively inexpensive photocatalyst material photostability, natural abundance, and higher activity[1]. The TiO_2 included three phases, Rutile, Anatase and Brookite, The first two types of TiO_2 are both in a tetragonal structure while Brookite in a orthorhombic[2]. Rutile is more stable phases, as compare with Anatase and Brookite which metastable and effect with change of temperature to transformed for rutile phase. Anatase is the phase normally forming into the sol-gel method of syntheses. Brookite often observed as a result for preparation TiO_2 in an acidic medium with low temperature as a by-product[3].

Titanium dioxide by using appropriate light can use for many applications such as fuel cell[4], remove air and water pollutants[5], hydrogen production[6]. One of the most disadvantages of TiO_2 was reacted with limited UV-light[1], thus specific energy to make Semiconductors chemically active for redox reaction.

Many efforts were done to solve or make this materials work in more efficiency by decreases this limitation. All the efforts were depend on modifying the electronic band of semiconductor such as metal/nonmetal doping, photosensitization with dyes and coupling with secondary semiconductors. The moderate methods are combining TiO_2 with an adsorbent material.

The common material which used to make coupling effect between adsorption[7-15] and photocatalsis is the carbonaceous species such as mesoporous carbons[16], carbon nanofibers[17], graphenes[18,19] and Carbon Nanotubes

CNTs[20,21]. Carbon nanotubes as a new born for the science at 1991[22] behave excellent electron conductions, high surface areas and strong adsorption capacity[7]. Carbon nanotubes can be classified to single-walled carbon nanotubes (SWNT) and multi-walled carbon nanotubes (MWNT). The electrical properties determined by the chiral angle which decides the properties of CNTs may semiconducting or metallic.

The synthesis composite CNT/TiO_2 can be done by different techniques such as sol-gel, chemical vapor deposition, and electro-spinning methods[23-28]. All of these methods include coupling in-situ of CNT with TiO_2[26,29]. In this work TiO_2 out-situ addition by using specific type of TiO_2 Degussa which is consisting of 80% Anatase and 20% Rutile, with SWNTs and MWNTs. The activity of synthesis composites was measured by make degradation for Cobalamin ($C_{63}H_{88}CoN_{14}P$). Cobalamin, or vitamin B12, known as a complex compound of organometallic species which is distinguished by the cobalt atom in a Corrine rings.

The photocatalytic decolorization of dyes which was carried out in aqueous solution by using different types of catalysts including ZnO, TiO_2 (Degussa P25), TiO_2 (Hombikat UV100), TiO_2 (Millennium PC105), and M/TiO_2 , *etc.* using UVA or natural light source[30-38].

The results show that the activity of catalysts was sequence: ZnO > TiO_2 (Degussa P25)>TiO_2 (Hombikat UV100) > TiO_2 (Millennium PC105) > TiO_2 (Koronose 2073). The TiO_2 reduce in activity with SWNT and MWNT when the ratio of CNTs more than 5% in the degradation of phenol in aqueous solution under near-UV irradiation. The same result published in many literatures[39] confirm that and related that to prevent the penetration of light at high concentration of CNTs. The enhance in activity of TiO_2 by CNTs can be related to large effective surface area, in addition to excellent adsorbent and the abilities of CNTs to dispersion with different materials which prevent the agglomerations of synthesis composite.

In the present study, The degradation of Cobalamin in aqueous solution was investigated using the prepared composites 1%SWNT/TiO_2 and 1%MWNT/TiO_2. The effect of types CNTs on the physiochemical properties of TiO_2 was measured by using UV-vis reflectance, Raman spectroscopy, XRD, Fluorescence spectroscopy and Surface area (BET). The mineralization by using synthesis composites was tested by measured total organic carbon TOC for Cobalamin solution.

2-Experimental

2-1 Chemicals

MWNTs, and SWNTs used in this study were purchased from Aldrich. According to the product specifications, the two compounds were fabricated by chemical vapor deposition method. SWNT constancies of more than 90% carbon which consisted of 77% SWNTs, with diameter 0.7-1.1nm. While MWNTs 95% carbon nanotubes with mode diameter 5.5, and The TiO_2 sample was purchased from Degussa, Germany (TiO_2-P25). CyanoCobalamin $C_{63}H_{88}CoN_{14}O_{14}P$ purchased from Sigma with purities more than 98.5%.

2-2- Preparation of Binary composite

Before synthesis, binary composites CNTs were activated, by treating with a mixture of acid HNO_3/H_2SO_4 (1/3) with an ultrasonic water bath for 7 hours[40]. 1gm of TiO_2 was suspended in 100 mL of distilled water for 30 min using an ultrasonic water bath, then the desired weight of CNTs was added to suspension of TiO_2 using ultrasonic water bath. The solution containing the mixed suspension was filtered by using a vacuum evaporator (Rota vapor re121 BUSHI 461 water Bath) at 45 °C. After the water evaporated, the composite was dried overnight in an oven at 104 °C to avoid any physicochemical changes in the carbon materials that occur to higher temperatures in the presence of oxygen.

2-3- Measured the activity of composite

The photocatalytic activities of pristine TiO_2, 1%SWNT/TiO_2 and 1%MWNT/TiO_2 were determined by the decolorization of Cobalamin in an aqueous solution under UV light with light intensities 1.3 mW/cm^2. The catalysts (175m g) were suspended in 100 mL of 40 ppm Cobalamin solutions to a glass vessel. Prior to irradiation, the suspensions were magnetically stirred in the dark to ensure the establishment of an adsorption/ desorption equilibrium among the photocatalyst, Cobalamin and atmospheric oxygen, which was then considered as the initial concentration. The light irradiation of the reactor were done for 60 min and the removal

of the dispersed powders through centrifuge. The clean transparent solution was analyzed using an UV–Vis spectrophotometer. The spectra (300-700 nm) for each sample were recorded and the absorbance was determined at the characteristic wavelength at 550 nm. The TOC analysis were done by repeating the experiments for 8 hours with analyzed the clear sample every 2 hours.

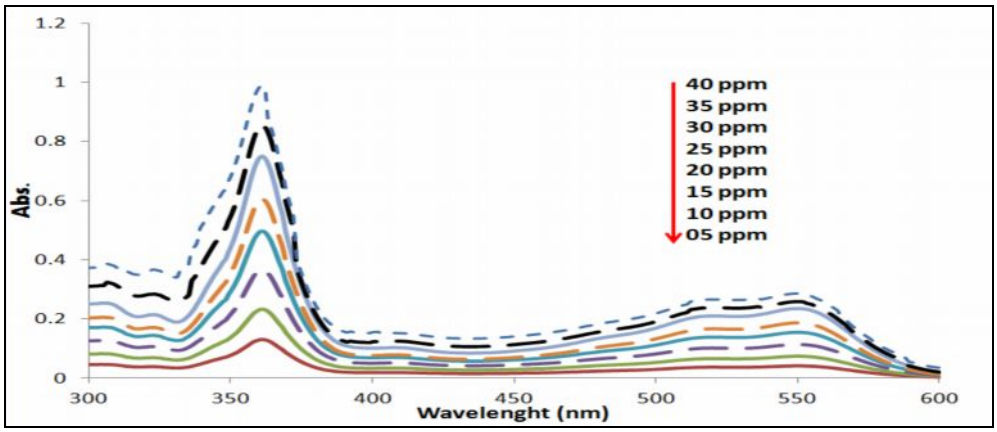

Figure 1. spectrum of UV-vis spectroscopy for Cobalamin with different concentrations.

3- Results and Discussion

3-1-Characterization of SWNT/TiO_2 and MWNT/ TiO_2

The UV-vis spectra were measured at room temperature in air on CARY 100 Bio UV-vis spectrophotometer equipped over the range from 200–800nm. $BaSO_4$ was used as a reflectance standard to measure UV-Vis diffuse reflectance spectra. The X-ray diffraction (XRD) patterns were measured on a (Rigaku Rotalflex, RU-200B) X-ray diffractometer using Cu Kα radiation (wavelength 0.15405 nm) with a Ni filter. The tube current was 100 mA with a tube voltage of 40 kV. The 2θ angular regions between 15 and 65° were explored at a scan rate of 5°/min. For all XRD tests, the resolution in 2θ scans was kept at 0.02° for all the measurements.

Raman analysis was done by using Sentara infinity 1 Bruker with using laser light at 530 nm, intensity 2 mW for 5 lops per 2s and resolution equal to 3-5 cm. Spectrofluorophotometer RF-540 Shimadzu was used to analyze the photoluminances for TiO_2 and composites in the range of 350-650 nm. The total organic carbon TOC was done by using TOC 5000A Shimadzu. Surface area estimation of the TiO_2 powders has been performed by the Brunauer-Emmett-Teller (BET) method, performed on a Micrometrics Automate 23 apparatus. The samples have been previously heated to 125 °C for 30 min to remove possible contaminants and humidity adsorbed on their surfaces. The measurements have been performed using a gas mixture containing 30 % N_2 and 70 % He. The band-gap energies E_g value was determined using the Kubelka–Munk function[25] of optical absorption for allowed direct transitions:

$$h\nu = A\,(h\nu - E_g)^{1/2}$$

Where A is the absorption coefficient and (hν) is the discrete photon energy. The value of band gap energy (E_g) can be calculated from diffuse reflectance data. The extrapolating linear portion of the $(FR \times h\nu)^{1/2}$ vs hν curves to FR = 0 which refer to the value of E_g band gap.

The most important consideration that TiO_2 absorbance occurred below 400 nm, whereas for SWNTs and MWNTs broad peaks of absorption can be observed between 450-1000 nm. Figure 1 shows the UV-Vis diffuse reflectance spectra of CNT/TiO_2 composites. The red shift of absorbance for composites in UV- light region due to: ascribed to intrinsic property of CNTs, inhomogeneous mixing between TiO_2 and CNTs which can act as excellent carrier electrons[41].

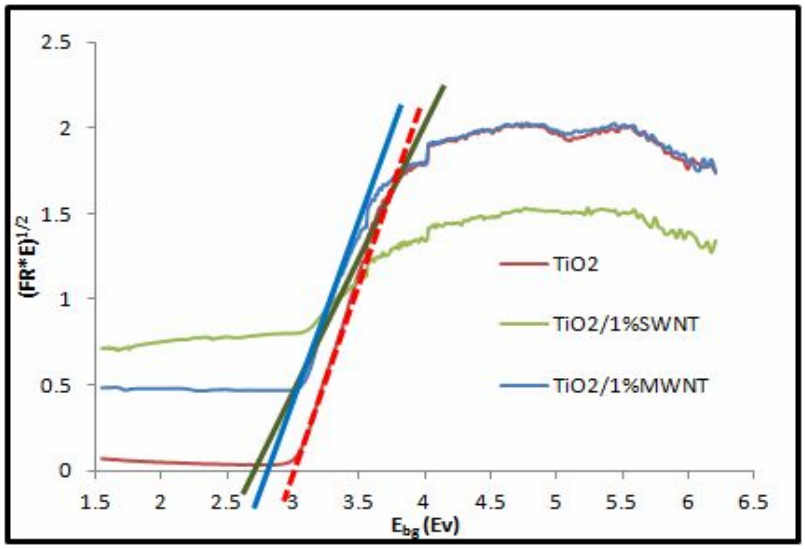

Figure 1.Band gap for TiO_2 , TiO_2/1%SWNT , TiO_2/1% MWNT .

The X-ray diffraction (XRD) patterns were used to tested the agglomerations estimation byline broadening measurements in the Debye–Scherrer equation[37].

$$d = K \lambda / \beta \cos\theta$$

Where d is the average crystallite size, λ is the X-ray wavelength in nanometer (nm) and that equal to (0.15405 nm), β is the peak width of the diffraction peak profile at half maximum height resulting from small crystallite size in radians and K is a constant related to crystallite shape mostly equal to 0.9. The peaks at 25.3° and 27.4° are the characteristic reflection for anatase and rutile, respectively for TiO_2.

Figure.2 shows the characteristic peaks of CNTs appears at $2\theta=25.9^o$ and 43.2^o, due to diffraction from C (100) and C (002) planes of the carbon nanotubes[42].

Figure.3 for pristine and modifying TiO_2 with SWNTs and MWNTs The first peak disappears in binary composites because the overlapped for these peak with the anatase peak of TiO_2 at 25.9^o[31]. The second peak of CNTs seem weak and increase in intensity with change the type of CNTs, which is larger within SWNTs as compare with MWNTs. The result shows that agglomerations of compound significantly affected by CNTs when reduce in exist of SWNTs more than MWNTs[43].

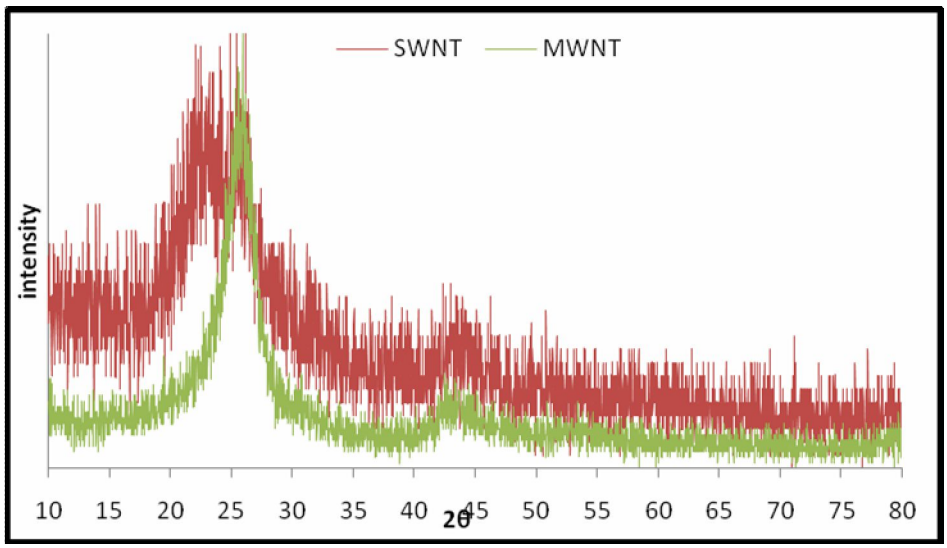

Figure 2.The XRD patterns for SWNT and MWNT

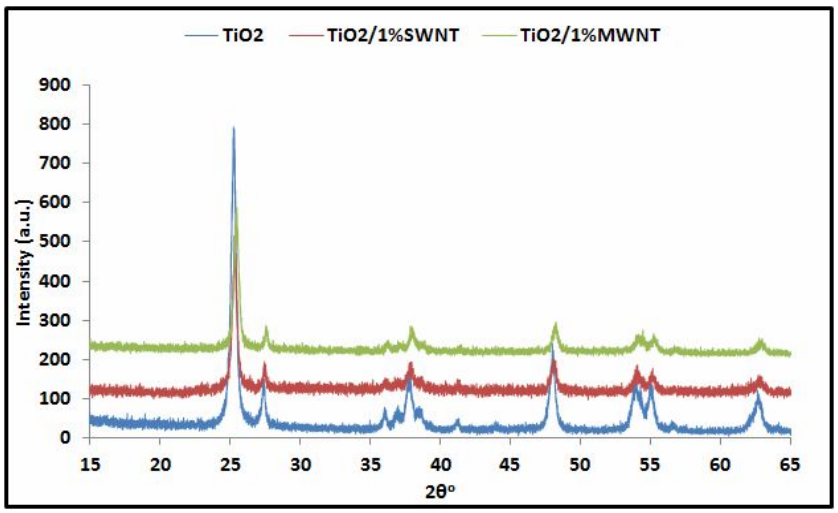

Figure 3.The XRD patterns for pristine and modify TiO_2 with SWNT and MWNT

The Raman spectra in Figure.4 show Both spectra G band at 1582 cm^{-1} corresponding to the -C-C- bond in the wrapped graphene plane, and D band at 1330 cm^{-1} corresponding to the C-related defects of SWNT and MWNTs. The 2D and G+D bands were typical shown for the two types of CNTs[7].

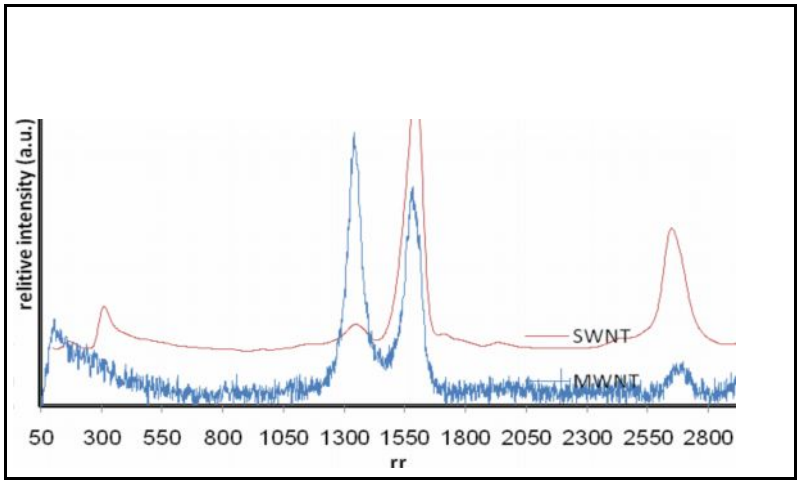

Figure 4. Raman shift for SWNTs and MWNTs .

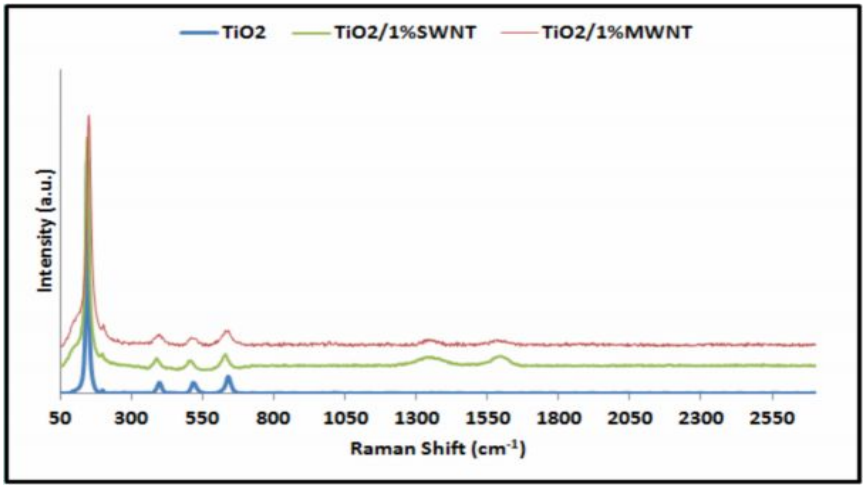

Figure 5. Raman shift for Pristine TiO_2, 1%SWNT/ TiO_2 and 1%MWNT/ TiO_2.

From Figure.5 the peaks in the 100-700 cm^{-1} region confirmed the presence of anatase TiO_2 with a dominating at 150 cm^{-1} (E_g), 395.1 cm^{-1} (B_{1g}), 512.5 cm^{-1} ($A_{1g} + B_{1g}$) and 636.7 cm^{-1} (E_g), respectively. The rutile phase at 143, 235 cm^{-1} which refer to the B_{1g}, two-phonon scattering, 445 cm^{-1} E_g, and 612 cm^{-1} A_{1g}, respectively[44]. In the case of 1% CNT/TiO_2 composites, all the Raman bands for anatase still remain with slightly broadened as compared to the pure TiO_2. The slight blue-shift of peaks relative to acid-treated of CNTs, refer to the interfacial interaction between TiO_2 and acid-treated CNTs. The shift was more for SWNTs than MWNTs which agree with their decrease in agglomerations as shown in Table 1. In addition, it is noteworthy the peaks assigned to SWNTs within the composites exhibit broadening and more clear as compare with composite which include MWNTs[45] due to real connections' across the interface between CNTs and TiO_2, not just mere mixture[46].

Photoluminescence, PL, spectroscopy was used to determine the possibility of charge carrier trapping, immigration, transfer, separation, and recombination holes e^-/h^+ in semiconductor[47]. Figure.6 for PL spectra of pristine TiO_2 nanoparticles,1%SWNT/TiO_2 and1% MWNT/TiO_2 nanohybrids which all feature a broad blue emission at 384nm and 479 nm under an excitement wavelength of 320 nm.

An emission peak at 384 nm corresponds to a direct band emission, the Fundamental band gap of 3.18 eV of TiO_2. The emission peak at 479 nm associates to the emission process related to the presence of oxygen vacancy defect in TiO_2. The intensity of these peaks is proportional to the possibility of such emission processes to occur.

The CNTs behave an important roles to act as an electron reservoir to trap electrons emitted from TiO_2 particles, which result in hindering electron-hole pair recombination. The shifts of peak is like a result for the trapping of the electrons at the active site of composite[45]**.** The composites showed reduces in PL intensity which refer to reduce in charge recombination for composite with SWNTs more than the composite that contains for MWNTs. This refer to new evidence of the better attachment for the SWNT/TiO_2 than MWNT/TiO_2[48].

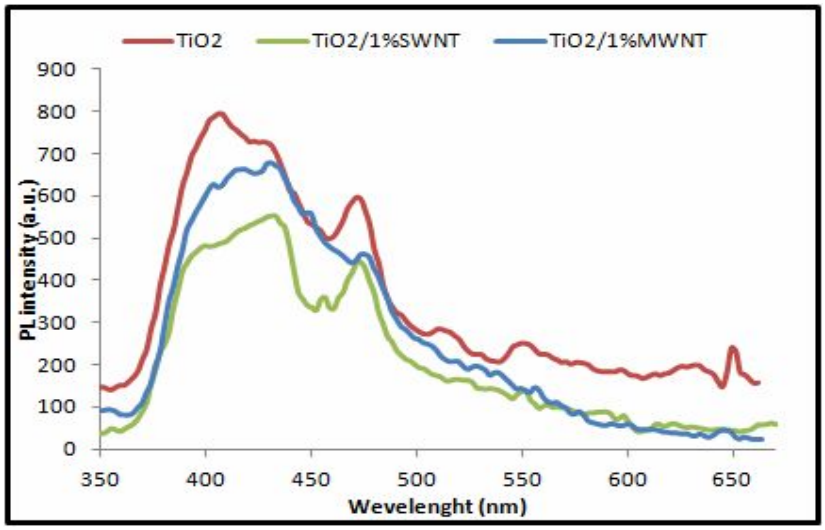

Figure 6. Flurecences spectra for TiO_2, TiO_2/1%SWNT and TiO_2/1%MWNT

The value of surface area shows interesting results when TiO_2/1%SWNT has less value as compare with TiO_2/1%MWNT. The interesting related to 1282 m^2/g for SWNTs while 238 m^2/g for MWNTs, which may refer to higher distribution for SWNTs in TiO_2 and strong connections.

Effect of CNTs on the adsorption property of TiO_2

The adsorption dynamics for the Cobalamin with TiO_2 and the two types of synthesis photocatalysts composite are shown in Figure.7, results shows that the amount of the Cobalamin adsorbed onto photocatalyst increases with the composite TiO_2/1%MWNT more than TiO_2/1%SWNT and pristine TiO_2 which can be arranged as the following: TiO_2/1%MWNT>TiO_2/1%SWNT>TiO_2

The equilibrium was achieved within 30 min for the three photocatalysts. Although surface area for MWNTs was less than SWNTs, but the interesting was MWNT/TiO_2 more active for adsorption. This result obtained in many literatures which deals with synthesis of binary composite for TiO_2 and CNTs[49]. This behavior may be related to the Small internal diameter for SWNTs then MWNTs with large size of the molecule Cobalamin which limited the adsorption within SWNTs.

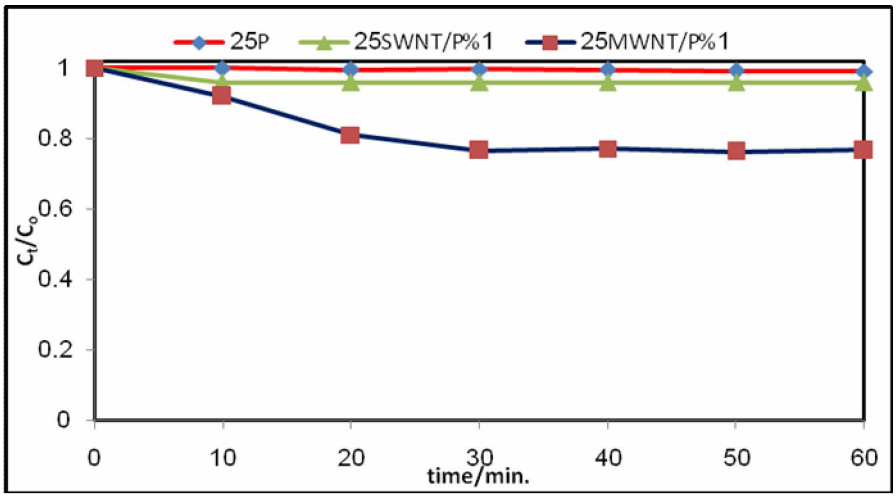

Figure 7. dark reaction for TiO_2, TiO_2/1%SWNT and TiO_2/1%MWNT with, 40ppm Cobalamin at 298K

The activities of adsorption was agree with the results of surfaces areas for synthesis composites.

3-3-Effect of CNTs on the photodegradation of Cobalamin with TiO_2

The photolysis of Cobalamin without catalyst shows that the sources of illumination did not make any photolysis for Cobalamin. The decolorization process of Cobalamin by pristine TiO_2 and the two types of synthesis composite as a photocatalyst shows clear changes in activity. The decolorization activity of TiO_2 increases greatly in existent of CNTs, especially MWNTs which enhance the adsorption more than SWNTs as shown in Figure 8.

The photodegradation experiments by UV irradiation of the Cobalamin solutions follow the pseudo-first-order kinetics with respect to the concentration of dyestuff in the bulk solution (C):

$$-\frac{dC}{dt} = K_{app}\, C$$

When made Integration for this equation and by using the same restriction of $C = C_0$ at $t = 0$, and C_0 being the initial concentration in the bulk solution before starting the light reaction, thus the equation become

$$\ln\left(\frac{C_0}{C}\right) = K_{app}\, t$$

where K_{app} is the apparent reaction rate constant. A plot of ln (C_0/C) versus t for Cobalamin degradation with different composite of SWNT/TiO_2 and MWNT/ TiO_2 photocatalysts is shown in Figure 3. The value of K_{app} can be obtained directly from the slope of the respective linear curves in the Figure 9. Comparing the K_{app} for the photodegradation of Cobalamin with TiO_2 and the two types of composites.

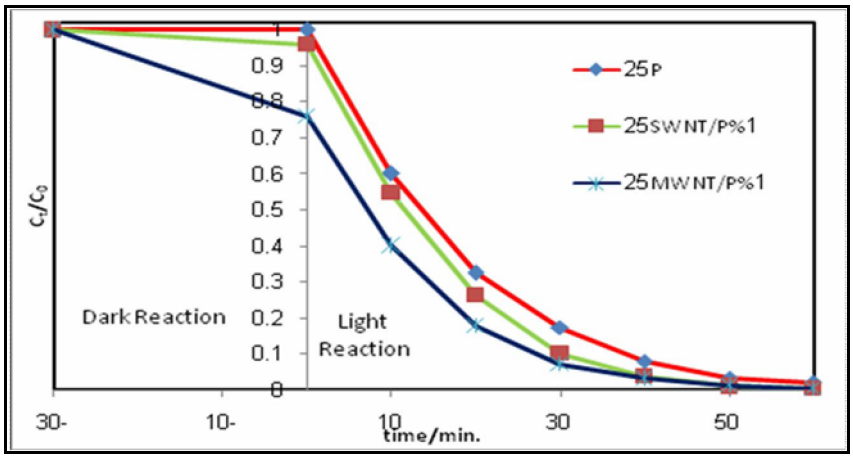

Figure 8. Degradation reaction for (175mg) pare TiO_2,1%SWNT/ TiO_2, and 1%MWNT/ TiO_2 with 40 ppm Cobalamin at 298K in exist of O_2 gas and light intensities 1.3 m W/cm^2.

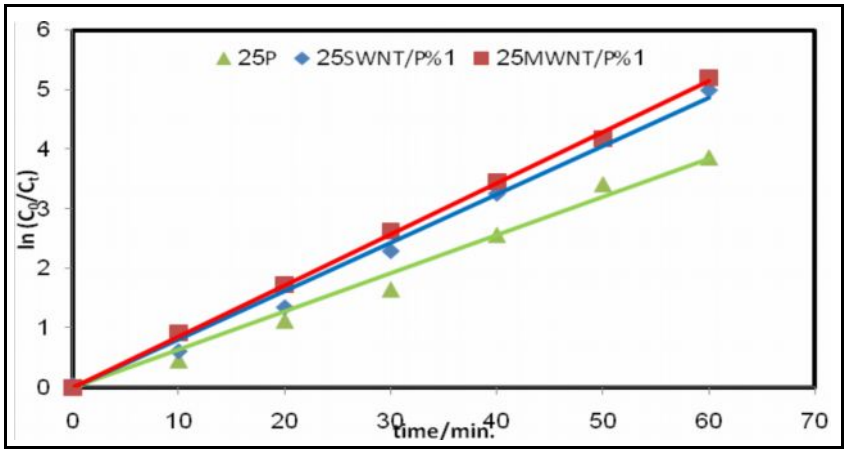

Figure 9. The changes in ln(C_0/C_t) with adsorption time for TiO_2, 1%SWNT/ TiO_2 and 1%MWNT/ TiO_2,with40ppm Cobalamin at 298K in exist of O_2 gas and light intensities 1.3 m W/cm^2.

Table 1.Sumary of UV- light photodegradation of Cobalamin on pristine and two composites of CNT/ TiO_2.

TOC_{8h}	**R**	**K/s^{-1}**	**C_0**	**Band gab/e V**	**S_{BET} (m^2/g)**	**Sample**
79.12	1	**0.0648**	≈40	**3.18**	**51**	TiO_2
88.28	1.25	**0.0811**	38.39	**2.85**	**71**	TiO_2/1%SWNT
90.37	1.31	**0.0851**	31.14	**2.9**	**80**	TiO_2/1%MWNT

The synergy factor (R) is expressed as the following equations

$R = k_{app}$ (TiO_2/ CNT)/ k_{app} (TiO_2)

when k_{app} (TiO_2/ CNT) , k_{app} (TiO_2) refer to the apparent rate constant for decolorization in exist of composite and TiO_2 respectively[50]. the CNTs causing increased in decolorization rate that attributed to increased the ability of adsorption for TiO_2 in exist of CNTs in composite. The exists of SWCNTs into TiO_2 matrix causing a new creates for kinetic synergetic effect more than MWCNTs. The adsorption abilities of MWCNTs reduced the color of Cobalamin before illumination but the SWNT win the competition after the illumination. Table 1 shows the value of adsorption at the equilibrium in dark reaction which represent starting point for

decolorization process with three compounds. The last action may related to the strong interaction between SWNTs and TiO_2 which enhance photocatalytic activity for SWNT/TiO_2 more than MWNT/TiO_2.

A proposed mechanism for the enhanced the photocatalysis of composites are shown schematically in Figure10.

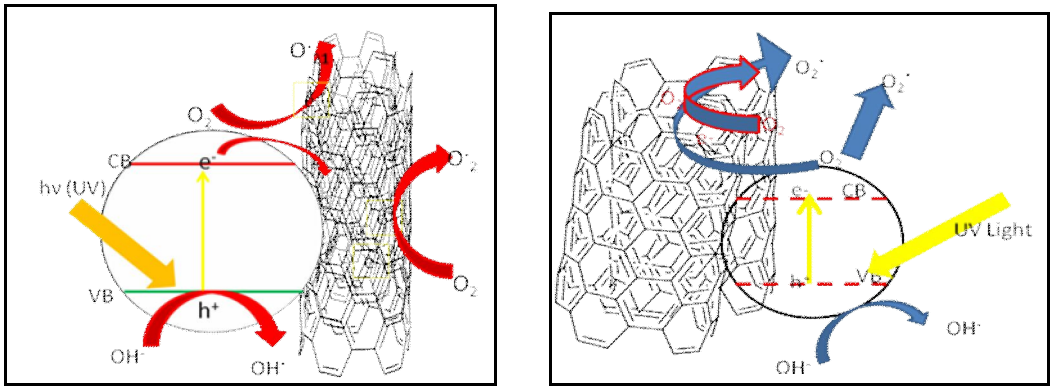

Figure 10. Schematic of a proposed model for TiO_2/SWNT and TiO_2/MWNT mechanisms.

Under UV illumination electrons are excited from valances band to the conduction band of the TiO_2, that leads to forming positive hole h^+ in valance band and negative charge in conduction band e^-. Most of these two charges will recombination quickly with losing many site which may react chemically, only <1% of electron and hole will react[51]. When CNTs attached to the surfaces of TiO_2 the exited electron in the conduction band of TiO_2 will be transfer to the surfaces of CNTs. This will allowing for separation and prevent or at least reduces the recombination process for the charges[52].

The last process will lead to increase the live time for the hole which forming $^{\cdot}OH$ in high concentration and the exited electron will react with O_2 gas to forming superoxide $O_2^{\cdot}$. The addition of small quantities CNTs to the semiconductors causing: i- changes on conductivity[53] which explained change in activity for TiO_2, ii- reduce the agglomerations of TiO_2 in binary composites which lead to appear more active site. Thus the e^-/h^+ will arrange in two side: the e^- on the surfaces of CNTs more ability to accept the electrons, then TiO_2. The h^+ or the positive charge stay without electron for more time (equation 1). The new active distribution of charge start to produce free radical, the first $O_2^{\cdot}$ forming when the e^- react with O_2 (equation 2). The second represents by reacting hydroxide ion with h^+ which produce $^{\cdot}OH$ (equation 3).

$$\mathbf{TiO_2/CNT + h\upsilon \rightarrow TiO_2^{h+VB} / CNT^{e-CB}} \quad \mathbf{(1)}$$

$$\mathbf{TiO_2^{h+VB} / CNT^{e-CB} + O_2 \rightarrow O_2^{\cdot} + TiO_2^{h+VB} / CNT} \quad \mathbf{(2)}$$

$$\mathbf{TiO_2^{h+VB} / CNT + {}^{-}OH \rightarrow {}^{\cdot}OH + TiO_2 / CNT} \quad \mathbf{(3)}$$

The band gab for TiO_2 about 3.18 e V and the band gap for MWNTs which 0.5 eV while less than 0.1 eV for SWNTs. The higher conductivity of SWNTs as compare with MWNTs make the equation 1 and 2 faster for SWNT/TiO_2 then MWNT/TiO_2 which explain the higher activity with SWNTs. The abilities of MWNTs with TiO_2 were more active to remove Cobalamin color than SWNTs in the dark reaction. Table 1 shows contrast to adsorption and mineralization through decolorization. The interesting in contrast may relate to ability of SWNTs to remove the electrons from TiO_2 more than MWNTs thus the degradation was more active with SWNTs.

To test the ability for reuse synthesis composite, the two types of composite was tested for three times which were shows a good efficiency for the recycling TiO_2/1%SWCNT and TiO_2/1%MWCNT photocatalysts.

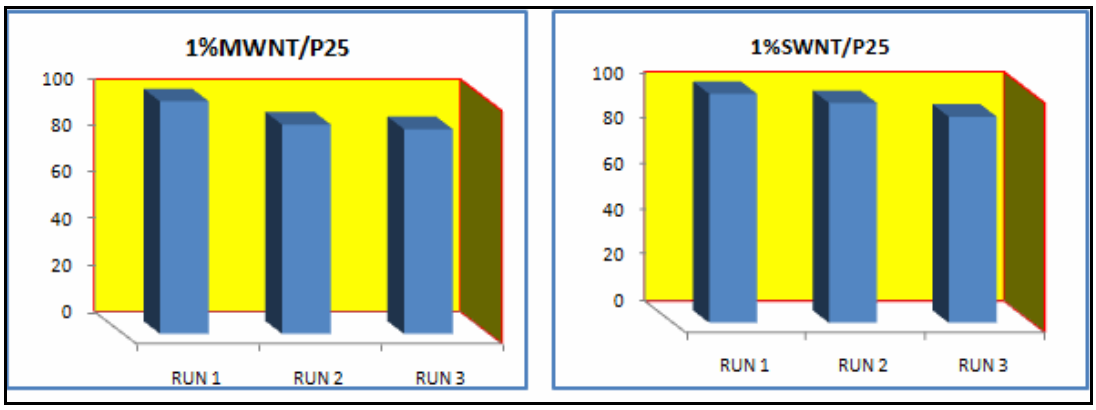

Figure 11. The efficiency of two composites to reuse there times.

4-Conclusions

The coupling effect of adsorption/photocatalitc which accrued between carbon nanotubes by using CNTs with TiO_2 had represented the key of high efficiency for decolorization and mineralization for Cobalamin. This study demonstrates three important points: the first is the charge transfer is very sensitive and effected by the types of carbon nanotubes. The second increase the ability of the new synthesis composite on the adsorption as comparing with pristine semiconductor did not consider only condition that enhance the activity. The third a good conductivity mostly gives a clear variation in potency. In this case SWNTs appear more abilities to make enhanced in activity of TiO_2 as comparing with MWNTs. The presence of carbon nanotubes, along TiO_2, is significant, since they have not been observed or rare by compare for adsorption and mineralization throw decolorization.

References:

1. Hoffmann, M. R.; Martin, S. T.; Choi, W.; Bahnemann, D. W., 1995. Environmental Applications of Semiconductor Photocatalysis Chem. Rev., 95: 69-96
2. Sai, G., , and Bang-Gui, L., 2012. Electronic structures and optical properties of TiO2: Improved density-functional-theory investigation, Chin. Phys. B 21: 057104 (057101-057107).
3. Di Paola, A., , Bellardita, M., and Palmisano, L., 2013. Brookite, the Least Known TiO2 Photocatalyst, Catalysts, 3: 36.
4. Drew, K.; Girishkumar, G.; Vinodgopal, K.; Kamat, P. V., 2005. Boosting Fuel Cell Performance with a Semiconductor Photocatalyst:â€‰ TiO2/Ptâ^'Ru Hybrid Catalyst for Methanol Oxidation, The Journal of Physical Chemistry B, 109: 11851-11857.
5. David F. Ollis, and Craig Turchi, 1990. Heterogeneous photocatalysis for water purification: Contaminant mineralization kinetics and elementary reactor analysis, Environmental Progress, 9: 229–234.
6. Liao, C., , Huang, C., and Wu, J. C. S., 2012. Hydrogen Production from Semiconductor-based Photocatalysis via Water Splitting, Catalysts, 2: 490-516.
7. Alkaim A. F., Sadik Z., Mahdi D. K., Alshrefi S. M., Al-Sammarraie A. M., Alamgir F. M., Singh P. M., and Aljeboree A. M., 2015. Preparation, structure and adsorption properties of synthesized multiwall carbon nanotubes for highly effective removal of maxilon blue dye, Korean J. Chem. Eng., 32: 2456-2462.
8. Aljeboree A. M., Alkaim A. F., and Al-Dujaili A. H., 2015. Adsorption isotherm, kinetic modeling and thermodynamics of crystal violet dye on coconut husk-based activated carbon, Desalin. Water Treat., 53: 3656-3667.
9. Hadi Z. A., Aljeboree A. M. and Alkaim A. F., 2014. Adsorption of a cationic dye from aqueous solutions by using waste glass materials: isotherm and thermodynamic studies, Int. J. Chem. Sci., 12: 1273-1288.
10. Alkaim A. F., Aljeboree A. M., Alrazaq N. A., Baqir S. J., Hussein F. H., and Lilo A. J., 2014. Effect of pH on Adsorption and Photocatalytic Degradation Efficiency of Different Catalysts on Removal of Methylene Blue, Asian Journal of Chemistry, 26: 8445-8448.

11. Aljeboree A. M., Radi N., Ahmed Z., and Alkaim A. F., 2014. The use of sawdust as by product adsorbent of organic pollutant from wastewater: adsorption of maxilon blue dye, Int. J. Chem. Sci., 12: 1239-1252.
12. Aljeboree A. M., Alshirifi A. N., and Alkaim A. F., 2014. Kinetics and equilibrium study for the adsorption of textile dyes on coconut shell activated carbon, Arabian J. Chem., 10.1016/j.arabjc.2014.01.020.
13. Alkaim A. F., and Alqaragully M. B. , 2013. Adsorption of basic yellow dye from aqueous solutions by Activated carbon derived from waste apricot stones (ASAC): Equilibrium, and thermodynamic aspects, Int. J. Chem. Sc., 11: 797-814.
14. Aljeboree A. M., 2015. Adsorption of methylene blue dye by using modified Fe/Attapulgite clay., Research Journal of Pharmaceutical, Biological and Chemical Sciences 6: 778-788.
15. Aljebori, A. M.; Alshirifi, A. N., 2012. Effect of Different Parameters on the Adsorption of Textile Dye Maxilon Blue GRL from Aqueous Solution by Using White Marble, Asian journal of chemistry, 24: 5813-5816
16. Ren, W.; Ai, Z.; Jia, F.; Zhang, L.; Fan, X.; Zou, Z., 2007. Low temperature preparation and visible light photocatalytic activity of mesoporous carbon-doped crystalline TiO2, Applied Catalysis B: Environmental, 69: 138-144.
17. Yang, Z.; Du, G.; Meng, Q.; Guo, Z.; Yu, X.; Chen, Z.; Guo, T.; Zeng, R., 2012. Synthesis of uniform TiO2@carbon composite nanofibers as anode for lithium ion batteries with enhanced electrochemical performance, Journal of Materials Chemistry, 22: 5848-5854.
18. He H.-Y., Fei J., and Lu J., 2015. High photocatalytic and photo-Fenton-like activities of ZnO-reduced graphene oxide nanocomposites in the degradation of malachite green in water, Micro & Nano Letters, IET, 10: 389 - 394.
19. Wang, G. C. Y. Z. H. K. T. H. Y., 2014. Hydrothermal synthesis of TiO2/reduced graphene oxide nanocomposite with enhanced photocatalytic activity, Micro & Nano Letters, IET: Year: 2014, Volume: 2019, Issue: 2012 Pages: 2932 - 2934, DOI: 2010.1049/mnl.2014.0238.
20. Yanga J., Hua X., and Zhang J., 2010. Voltammetric monitoring photodegradation of EDTA based on carbon nanotubes-modified electrode, Journal of Hazardous Materials, 181: 742-746.
21. Dai, K.; Zhang, X.; Fan, K.; Zeng, P.; Peng, T., Multiwalled Carbon Nanotube-TiO2 Nanocomposite for Visible-Light-Induced Photocatalytic Hydrogen Evolution, Journal of Nanomaterials, 2014: 8.
22. Iijima, S., 1991. Helical microtubules of graphitic carbon, Nature, 354: 56-58.
23. M. A. Salam, R. M. El-Shishtawy, A. Y. Obaid, 2014. Synthesis of magnetic multi-walled carbon nanotubes/magnetite/chitin magnetic nanocomposite for the removal of Rose Bengal from real and model solution, J. Ind. Eng. Chem., 20: 3559-3567.
24. V. K. Gupta, S. Agarwal, T. A. Saleh, 2011. Synthesis and characterization of alumina-coated carbon nanotubes and their application for lead removal, J. Hazard. Mater., 185: 17-23.
25. Dervishi, E.; Li, Z.; Watanabe, F.; Xu, Y.; Saini, V.; Biris, A. R.; Biris, A. S., 2009. Thermally controlled synthesis of single-wall carbon nanotubes with selective diameters, Journal of Materials Chemistry, 19: 3004-3012.
26. Yao, Y.; Li, G.; Ciston, S.; Lueptow, R. M.; Gray, K. A., 2008. Photoreactive TiO2/Carbon Nanotube Composites: Synthesis and Reactivity, Environmental Science & Technology, 42: 4952-4957.
27. Manafi, S., Nadali, H., and Irani, H. R., 2008. Low temperature synthesis of multi-walled carbon nanotubes via a sonochemical/hydrothermal method, Mater. Lett., 62: 4175-4176.
28. Sun Z., Zhang X., Na, Liu Z., Han B., and An G., 2006. Synthesis of ZrO2-Carbon Nanotube Composites and Their Application as Chemiluminescent Sensor Material for Ethanol, J. Phys. Chem. B, 110: 13410-13414.
29. Chen J., Luo H., Shi H., Li G., and An T., 2014. Anatase TiO2 nanoparticles-carbon nanotubes composite: Optimization synthesis and the relationship of photocatalytic degradation activity of acyclovir in water, Applied Catalysis A: General, 485: 188-195.
30. Mashkour M. S., Al-Kaim A. F., Ahmed L. M., and Hussein F. H., 2011. Zinc oxide assisted photocatalytic decolorization of reactive red 2 dye, Int. J. Chem. Sc., 9: 969-979.
31. Alrobayi E. M., Algubili A.M., Aljeboree A. M., Alkaim A. F., and Hussein F. H., DOI: 10.1080/02726351.2015.1120836. Investigation of Photocatalytic Removal and Photonic Efficiency of Maxilon Blue Dye GRL in the Presence of TiO2 Nanoparticles, Particulate Science and Technology.

32. Karam F. F., Kadhim M. I., and Alkaim A. F., 2015. Optimal conditions for synthesis of 1, 4-naphthaquinone by photocatalytic oxidation of naphthalene in closed system reactor, Int. J. Chem. Sci., 13: 650-660.
33. Alkaim, A. F., Dillert, R., & Bahnemann, D. W., 2015. Effect of polar and movable (OH or NH2 groups) on the photocatalytic H2 production of alkyl-alkanolamine: a comparative study, Environ. Technol., 36: 2190–2197.
34. Algubili A. M., Alrobayi E. M., and Alkaim A. F., 2015. Photocatalytic degradation of remozal briliant blue dye by ZnO/UV process, Int. J. Chem. Sci., 13: 911-921.
35. Kandiel T. A., Robben L., Alkaim A., and Bahnemann D., 2013. Brookite versus anatase TiO_2 photocatalysts: phase transformations and photocatalytic activities, Photochem. Photobiol. Sci., 12: 602-609.
36. Alkaim, A. F.; Kandiel, T. A.; Hussein, F. H.; Dillert, R.; Bahnemann, D. W., 2013. Enhancing the photocatalytic activity of TiO2 by pH control: a case study for the degradation of EDTA, Catal. Sci. Technol., 3: 3216–3222.
37. Alkaim A. F., Kandiel T. A., Hussein F. H., Dillert R., and Bahnemann D. W., 2013. Solvent-free hydrothermal synthesis of anatase TiO2 nanoparticles with enhanced photocatalytic hydrogen production activity, Appl. Catal. A-Gen, 466: 32-37.
38. Alkaim A. F., and Hussein F. H., 2012. Photocatalytic degradation of EDTA by using TiO_2 suspension, Int. J. Chem. Sci., 10: 586-598.
39. Kamil, A. M.; Hussein, F. H.; Halbus, A. F.; Bahnemann, D. W., 2014. Preparation, Characterization, and Photocatalytic Applications of MWCNTs/TiO2 Composite, International Journal of Photoenergy, Volume 2014, Article ID 475713: 8.
40. Wepasnick K. A., Smith B. A., Schrote K. E., Wilson H. K., Diegelmann S. R., and Fairbrother D. H., 2011. Surface and structural characterization of multi-walled carbon nanotubes following different oxidative treatments, Carbon, 49: 24-36.
41. Wang W., Serp P., Kalck P., and Faria J. L., 2005. Visible light Photodegradation of Phenol on MWNT-TiO2 Composite Catalysts Prepared by a Modified Sol-gel Method, J Mol Catal A Chem. , 235.
42. Akhavan O., Azimirad R., Safa S., and Larijani M. M., 2010. Visible light photo-induced antibacterial activity of CNT-doped TiO2 thin films with various CNT contents, Journal of Materials Chemistry, 20: 7386-7392.
43. Singh D. K., Iyer P. K., and Giri P. K., 2010. Diameter dependence of oxidative stability in multiwalled carbon nanotubes: Role of defects and effect of vacuum annealing, Journal of Applied Physics, 108: 084313.
44. 44. Liu G., Yan X., Chen Z.., Wang X., Wang L., Lu G. Q., and Cheng H.-M., 2009. Synthesis of rutile-anatase core-shell structured TiO2 for photocatalysis, Journal of Materials Chemistry, 19: 6590-6596.
45. Khan G., Kim Y.K., Choi S.K., Han D.S., Abdel-Wahab A., and Park H., 2013. Evaluating the Catalytic Effects of Carbon Materials on the Photocatalytic Reduction and Oxidation Reactions of TiO2, Bull. Korean Chem. Soc., 3: 1-8.
46. Dechakiatkrai C., Chen J., Lynam C., Min S.K., Kim S.J., Phanichphant S., and Wallace G.G., 2008. Direct Ascorbic Acid Detection with Ferritin Immobilized on Single-Walled Carbon Nanotubes, Electrochemical and SolidState Letters, 11: K4-K6.
47. Chen L., Zhang B., Qu M., and Yu Z., 2005. Preparation and characterization of CNT-TiO2 composites, Powder Technology, 154: 70-72.
48. Yu, Y.; Yu, J. C.; Chan, C.-Y.; Che, Y.-K.; Zhao, J.-C.; Ding, L.; Ge, W.-K.; Wong, P.-K., 2005. Enhancement of adsorption and photocatalytic activity of TiO2 by using carbon nanotubes for the treatment of azo dye, Applied Catalysis B: Environmental, 61: 1-11.
49. Matos J., Laine J. , and Herrmann J.-M., 1998. Synergy effect in the photocatalytic degradation of phenol on a suspended mixture of titania and activated carbon, Applied Catalysis B: Environmental, 18: 281-291.
50. Slimen H., Lachheb H., Qourzal S., Assabbane A., and Houas A., 2015. The effect of calcination atmosphere on the structure and photoactivity of TiO2 synthesized through an unconventional doping using activated carbon, Journal of Environmental Chemical Engineering, 3: 922-929.
51. Li G., and Gray K. A., 2007. The solid-solid interface: explaining the high and unique photocatalytic reactivity of TiO 2-based nanocomposite materials, Chemical physics, 339: 173-187.

52. Chen W., Fan Z., Zhang B., Ma G., Takanabe K., Zhang X., and Lai Z., 2011. Enhanced visible-light activity of titania via confinement inside carbon nanotubes, J Am Chem Soc., 133: 14896-14899.
53. Vajda K., Mogyorosi K., Nemeth Z., Hernadi K., Forro L., Magrez A., and Dombi A., 2011. Photocatalytic activity of TiO2/SWCNT and TiO2/MWCNT nanocomposites with different carbon nanotube content, Phys. Status Solidi B, 248: 2496-2499.

*****